

Static Strength and Buckling Analysis of an Aircraft Support

Daqian Zhang, Guoxiong Zhang* and Yueyang Chen 

College of Aerospace Engineering, Shenyang Aerospace University, Shenyang 110136, China; zhangdaqian65@163.com (D.Z.); chen Yueyang0520@163.com (Y.C.)

* Correspondence: zhangguoxiong@126.com; Tel.: +86-131-3812-2994

Abstract: At the initial stage of design, the structural strength and stability of the load-bearing structural members of the aircraft are mainly considered. In this paper, the structural strength and stability of a support of aircraft assembly are analyzed. First, structural strength analysis, under the design load of 30.151 KN, and numerical analysis shows that, in the stress concentration area, the stress peak value is 571.9 Mpa. The experimental value of the strain sensor S6 position is compared with the numerical results, and the error is within 2.5%, which verifies the validity of the numerical model and the structural strength to meet the design requirements. Second, structural stability adopts the method of buckling analysis. Linear buckling analysis shows that the first six order buckling modes and critical loads. The first order critical load is 464.9 KN. Risk arc length method is used in the nonlinear buckling analysis. Considering the geometric imperfection of the support, 1% and 10% initial imperfection values are used. Nonlinear buckling critical load values—without imperfection and considering the initial imperfection—are obtained, which are 110.6 KN, 108.4 KN, and 106.2 KN, respectively. There is little difference between the three values, indicating that the geometric imperfection of the support is not obvious to the nonlinear buckling, and they have structural stability. In the case of no imperfection, the maximum deformation of the main area reaches 21.4 mm, and the support enters the instability state. This paper comprehensively discusses the results of structural strength and structural stability analysis, which can provide reference for the design and optimization of bearing components.

Keywords: aircraft support; strength test; buckling analysis; structural strength optimization



Citation: Zhang, D.; Zhang, G.; Chen, Y. Static Strength and Buckling Analysis of an Aircraft Support. *Appl. Sci.* **2023**, *13*, 4362. <https://doi.org/10.3390/app13074362>

Academic Editor: Rosario Pecora

Received: 12 March 2023

Revised: 23 March 2023

Accepted: 24 March 2023

Published: 29 March 2023



Copyright: © 2023 by the authors. Licensee MDPI, Basel, Switzerland. This article is an open access article distributed under the terms and conditions of the Creative Commons Attribution (CC BY) license (<https://creativecommons.org/licenses/by/4.0/>).

1. Introduction

Both strength failure and buckling belong to the failure modes of aircraft structural components, especially in the main load-bearing components of aircraft. In order to avoid such failures, sufficient research and analysis must be carried out in the design stage [1]. International researchers have done significant research on these two aircraft components. Diltemiz [2] researched the failure of the oil cylinder bracket of the aircraft main landing gear, which revealed the cause of the local fracture of the bracket due to the high strength stress during overload. LI [3] analyzed the strength of the fuselage panel, studied the buckling of the panel by using static tests, and introduced pre-damage to study the effect of strain distribution. It is worth noting that they can provide the reference for structural optimization. As for structural optimization, the latest research involved a different approach. Aditya [4] using generative design in the main landing gear of an aircraft, and the final design of the main landing gear resulted in a 30% weight reduction. Spyridon [5] proposed a novel optimized framework using low-cost numerical tools in the design stages of aircraft wings. However, few studies have considered the combination of structural strength and stability to conduct a more comprehensive study of load-bearing components. In this paper, considering these two aspects, we study a support of load-bearing components of aircraft at the initial stage of design [6]. Strength analysis and buckling analysis are used to studying the structural strength and stability of aircraft

support, respectively. The method of research can provide a basis for studying bearing capacity and structural optimization design of aircraft support.

2. Methods

Structural strength design [7] is one of the most important parts of aircraft structure design [8]. The strength analysis, in this paper, includes both numerical calculation and strength test to verify whether the strength requirements are met. Structural strength test is an indispensable part of aircraft development. On the basis of HB 7713-2002 general requirements of static strength test for aircraft structure [9], we used the design load of 30.151 KN as the strength test load. In the strength test, it is necessary to reasonably select the loading mode of the test load, which should be the same as the real loading state of the aircraft [10]. The research object of this paper is the load-bearing assembly connected by the fuselage. Due to the complex geometry and loading conditions, the test fixture needs to be designed specifically.

As shown in Figure 1a, yellow frame area is the main bearing surface and the main loading area for strength analysis and buckling analysis. Connection of the support is shown in Figure 1b, where white area in the middle is a fixed connection, and the green area is an adjacent connector. In the strength test, considering the force of the connection in the aircraft, these two areas are considered as the fixed ends of the strength test. Yellow and blue areas are the loading parts of the support, which are considered as the loading end of the test fixture.

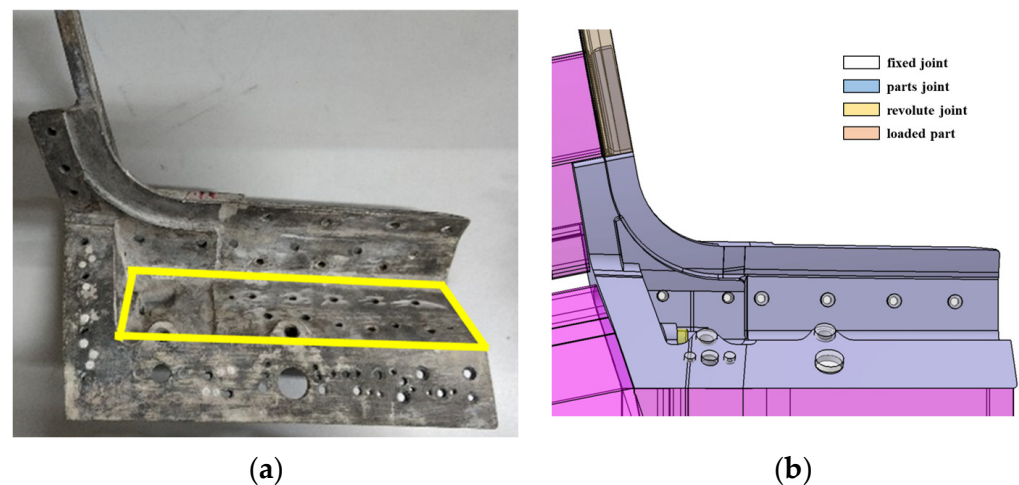


Figure 1. Connections on the fuselage. (a) Main loading area, (b) Connection of the support.

In this paper, buckling analysis is used to study the structural stability of bearing parts. The purpose of buckling analysis is to determine the critical load when the structure changes from a stable state to an unstable state. According to the size of the deformation state before instability, the linear analysis or nonlinear analysis before instability is used. In this paper, the eigenvalue method is used to analyze the linear eigenvalue buckling, and then, the first order critical load obtained by linear buckling is selected as the load reference value of nonlinear buckling analysis. Considering the case of geometric imperfections, 1% and 10% of the initial imperfection values are used, and the Riks arc length method is used to analyze the nonlinear buckling without imperfection and with initial imperfection, respectively. Based on the results of strength analysis and buckling analysis, this paper discusses its strength and instability to obtain its structural strength and structural stability, which can provide a basis for studying its bearing capacity and structural optimization design. The main process is shown in Figure 2.

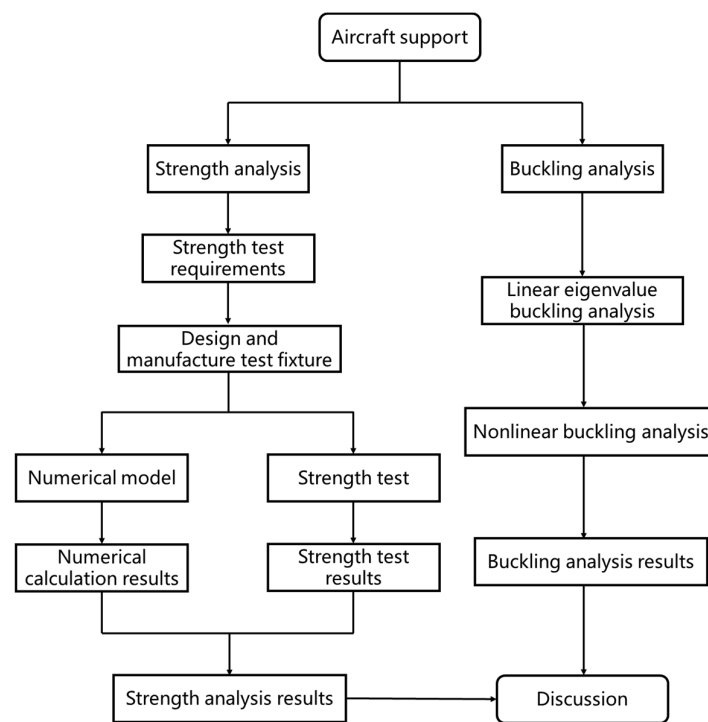


Figure 2. The main process.

3. Strength Test Fixture

The design of the test fixture is one of the links of the strength test [11]. It is necessary to design and manufacture the test fixture reasonably before the test. According to the general requirements of HB 7713-2002 for static strength test of aircraft structure, the strength test fixture is designed. In this paper, the stiffness of the test fixture material and the deformation generated in the test are considered. Influence on the test results should be as small as possible. Therefore, the fixture material should have significant stiffness. At the same time, it is also necessary to consider that the stiffness of the fixture gasket should be roughly the same as that of the test piece. If the difference is too large, it is easy to cause excessive local stress at the connection and cause damage to the test piece. Considering the design of the strength test, the fixture and gasket are in Figure 3, where a and b in Figure 3 are the loading end and the fixing end. The material is 30CrMnSiA structural steel of GB/T 3077-1988. The c and d in Figure 3 are gaskets, and the material is 2B06 aluminum alloy of GB/T 3190-2008.

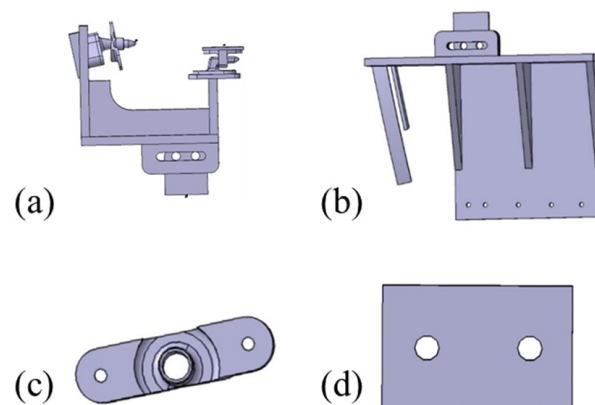


Figure 3. (a) Loading end, (b) the fixing end, (c,d) gaskets.

4. Strength Analysis

4.1. Numerical Analysis Model of Strength Analysis

Continuum mechanics describe object deformation by stress, strain, and displacement. These values are mainly considered in strength analysis. Their relationship can be described in an equation as follows:

$$\varepsilon = \frac{\Delta l}{l_0} \quad (1)$$

$$\sigma = E\varepsilon \quad (2)$$

where ε is strain, Δl is deformation, l_0 is initial length, σ is stress, and E is modulus of elasticity.

In this paper, the numerical analysis model is established before the test, and the geometric model established by CATIA is imported into HyperMesh. The model is mainly divided into hexahedral elements, and tetrahedral elements are used for some relatively complex structural areas. As shown in Figure 4, which is numerical analysis model, the main mesh size is 5 mm, and the model generates 114,253 nodes and 38,960 elements—the total elements used, as shown in Table 1. According to the requirements of fixture design, the material properties of each region of the mesh model are given, respectively. Table 2 shows the material parameters of the numerical model.

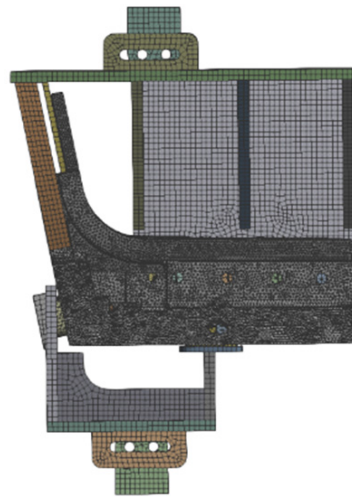


Figure 4. Numerical analysis model.

Table 1. The total elements used.

Part	Type	Shape	Amount
Fixture	3D Stress	Hex	23,844
Pad	3D Stress	Hex	1210
Support	3D Stress	Hex and Tet	13,906
			38,960

Table 2. The material parameters of the numerical model.

Part	E (GPa)	$\sigma_{0.2}$ (MPa)	σ_b (MPa)	μ
Fixture	200	835	1080	0.3
Pad	70	275	425	0.34
Support	71.7	540	582	0.33

The numerical analysis model of strength analysis created a step in Abaqus, and the procedure type of Static General was used. To view the actual situation of the strength test,

the boundary conditions of the numerical model are shown in Figure 5. The fixed parts of the fixture, at the fixed end, constrain the translational and rotational degrees of freedom in the three directions of XYZ. The loading part at the loading end applies a test load of 30.151 KN in the continuous tensile direction, while it constrains the other five degrees of freedom in the tensile direction. The connection between the test piece and the clamp is set with bolt contact. By establishing the above boundary setting, the situation of the strength test is fully simulated.

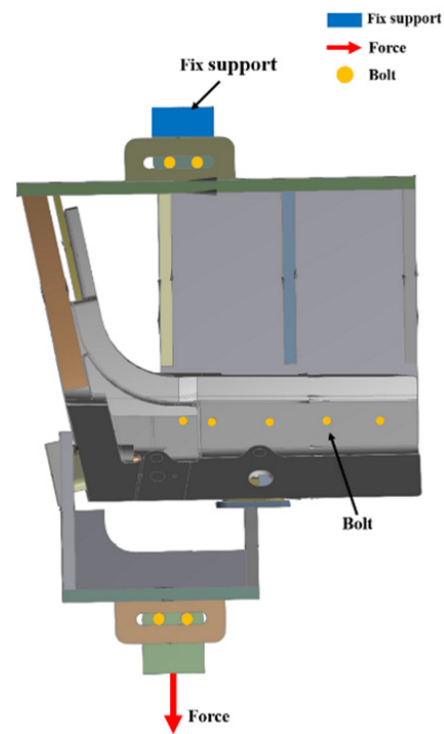
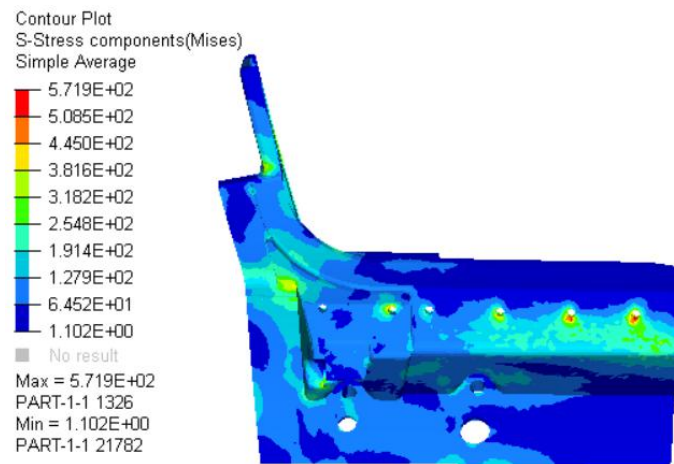


Figure 5. The boundary conditions of the numerical model.

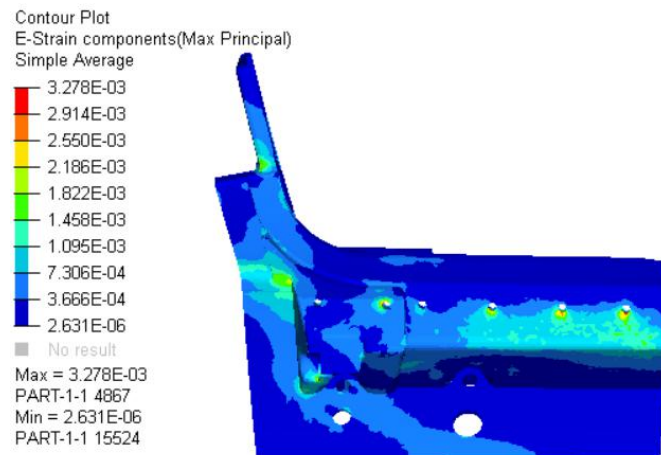
4.2. Numerical Results of Strength Analysis

The numerical results of strength analysis are shown in Figure 6a–c. The stress result, strain result, and displacement result under test load are shown, respectively. The stress concentration area appears in the left middle area of the test piece and the bolt connection. The stress concentration area at the bolt connection is more obvious. The stress range is 381.6–508.5 Mpa, mainly 425.3 Mpa, and the strain range is about 730.6 $\mu\epsilon$. The overall maximum displacement deformation is 5.104 mm, and the maximum stress is 571.9 Mpa, which is less than the tensile strength σ_b of the bearing part, and no strength failure occurs.

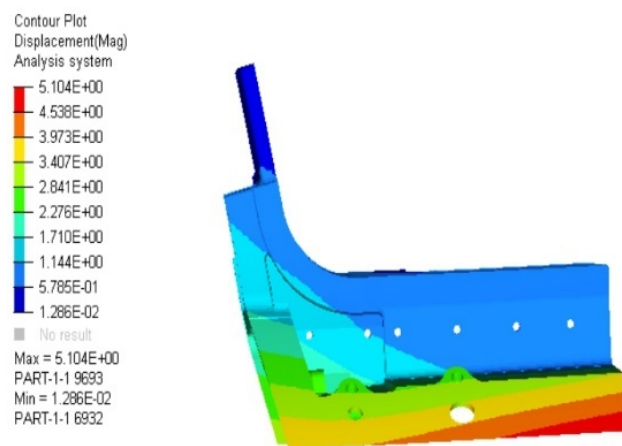
However, under the test load, the stress value of a small part of the area exceeds the yield strength $\sigma_{0.2}$ of the material, and it is mainly concentrated in the bolt connection between the test piece and the strength test fixture, accounting for 4.3% of the whole test piece, which does not affect the overall structural strength. The stress range of the main bearing area is 127.9–318.2 Mpa, which is less than the yield strength $\sigma_{0.2}$ of the material, indicating that the numerical analysis results of the test piece meet the strength design requirements. Through numerical results of strength analysis, there is the problem of yield strength in the connections of the test piece. Therefore, the further optimal design of structural strength can be mainly considered at the connection of the test piece.



(a)



(b)



(c)

Figure 6. (a) Stress result; (b) Strain result; (c) Displacement result.

4.3. Strength Test and Comparison

According to the force transmission characteristics and numerical analysis results of the test piece, the strength test confirms that the position of the test strain flower is S1~S6, as shown in Figure 7a. The strength test equipment is composed of a microcomputer-

controlled electronic universal testing machine (WDW-100E), a static strain test and analysis system (TST3822EN), and a strain gauge sensor (BA120-3AA150 (16)-G1K-JQC). The final test assembly is shown in Figure 7b.

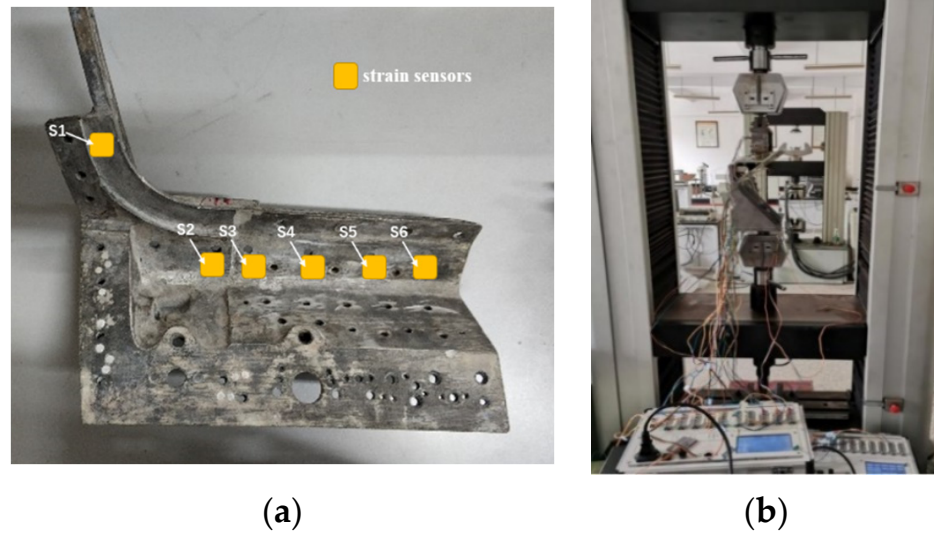


Figure 7. (a) The position of the test strain flower (b) strength test equipment.

In the aspect of load loading, 5% of the test load is taken as the first level, and the load is coordinated to 100% of the test load step by step. Load is maintained for 30 s, as shown in Table 3. The load loading process is then unloaded step by step to no load. During the test, as the load is gradually loaded, the test piece, as a whole, produces a small displacement deformation in the loading direction. In the process of step-by-step unloading of the load, the displacement deformation generated by the test piece disappears, and no obvious cracks or damage occur during the whole process. Finally, the strain curve under the test load is shown in Figure 8. The maximum test strain is 1577.9 $\mu\epsilon$ at the position of the strain sensor S6, and the strain values at the positions of the remaining strain sensors, S1 to S5, are 344.5 $\mu\epsilon$, 676.4 $\mu\epsilon$, 726.7 $\mu\epsilon$, 1378.1 $\mu\epsilon$, and 1199.9 $\mu\epsilon$, respectively. It shows that the strain situation of the area of the test piece gradually increased from left to right, and it relates to the thickness distribution of the test piece, where thickness on the left is greater than the thickness on the right.

Table 3. The load loading process.

Load/%	5	10	15	20	25	30	35	40
Value/N	1508	3015	4523	6030	7538	9045	10,553	12,060
Load/%	45	50	55	60	65	70	75	80
Value/N	13,568	15,076	16,583	18,090	19,598	21,106	22,613	24,121
Load/%	85	90	95	100				
Value/N	25,628	27,136	28,643	30,151				

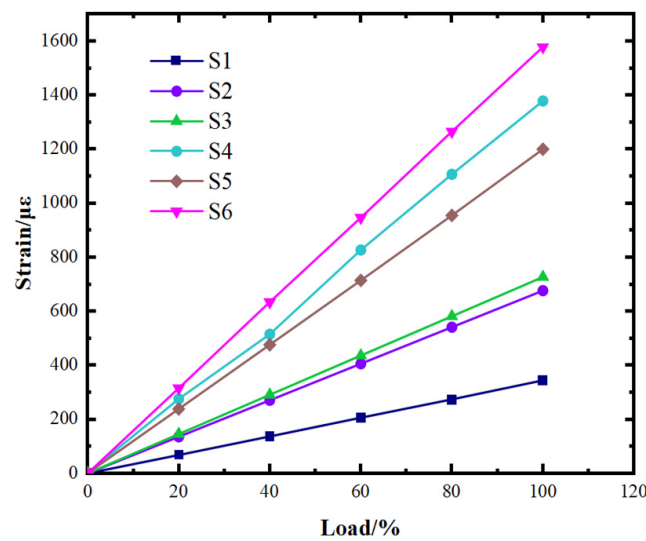


Figure 8. The strain curve under the test load.

The maximum strain of the S6 strain flower under test load is 1617.3 $\mu\epsilon$. Comparing the experimental values with the numerical analysis results, as shown in Figure 9, the error is within 2.5%, indicating the effectiveness of the numerical analysis model, and the structural strength of the test piece meets the requirements after the strength test. Through the results of the strength test, indicating strain of edge of the test piece is larger than other area. Therefore, the further optimal design of structural strength can be considered at the edge of the test piece.

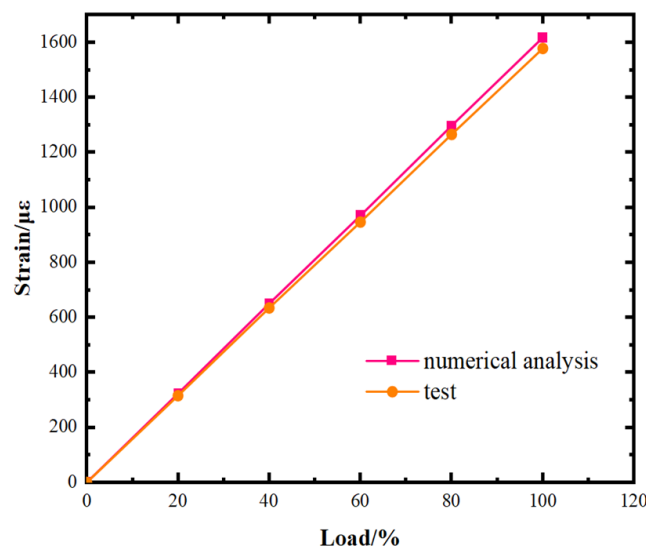


Figure 9. S6 comparing the experimental values with the numerical analysis results.

5. Buckling Analysis

The aircraft will be overloaded during take-off or landing [12], especially in the case of an emergency landing of large fuselage weight, which will undoubtedly bring a huge test to the load-bearing components of the aircraft. Through the buckling analysis, the structural instability of the bearing assembly under large load can be further obtained. In this paper, the buckling analysis is used to study the critical load of the main bearing area of the bearing assembly [13], as well as the instability of the bearing area when the critical load is applied. Buckling analysis includes linear eigenvalue buckling [14] analysis and nonlinear buckling analysis [15]. The linear eigenvalue buckling analysis does not consider the influence of geometric nonlinearity on the equilibrium equation and geometric equation [16], and it

solves the buckling mode and critical load of linear instability. The critical load can be used as the reference value of the nonlinear buckling analysis load [17]. Figure 10 shows the buckling analysis curve. The critical load point A is the linear eigenvalue buckling value, and the first peak point B of the solid curve is the nonlinear buckling value. The nonlinear buckling value is lower than the linear buckling value, which is generally about 40~60% of the linear buckling value. After reaching the first nonlinear buckling value, the structure will enter the instability region. Compared with linear buckling, nonlinear buckling is more accurate and in line with the actual situation.

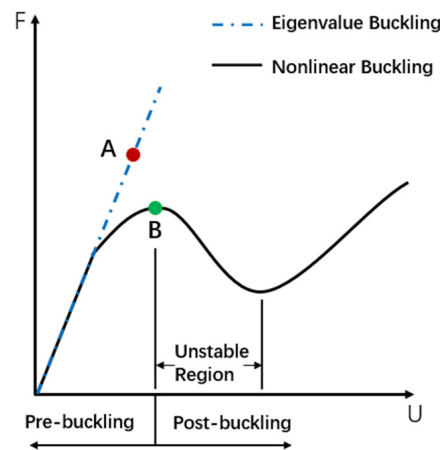


Figure 10. Buckling analysis curve. A is the linear eigenvalue buckling value, B is the nonlinear buckling value.

In this paper, the eigenvalue method is used to analyze the linear buckling of the aircraft bearing assembly. The eigenvalue of the first-order buckling mode is taken as the critical load, which is used as the reference value of the nonlinear buckling analysis load. In the linear buckling analysis, it is assumed that the material of the bearing assembly remains in an elastic state, and the relationship of eigenvalue buckling is as follow:

$$[\{K_e\} + \{\rho\}(\{K_u\} + \{K_G\})]\{\phi\} = 0 \tag{3}$$

where K_e is the elastic stiffness matrix of the structure, K_u is the initial displacement matrix, K_G is the initial stress matrix, ρ is the critical load, and ϕ is the displacement characteristic vector. Ignoring K_u , the characteristic equation of buckling stability analysis is obtained:

$$(\{K_e\} + \{\rho\}\{K_G\})\{\phi\} = 0 \tag{4}$$

Finally, considering the eigenvalues $\rho_1, \rho_2, \rho_3, \rho_4, \rho_5, \rho_6 \dots \dots$, the eigenvalue ρ_1 is the first-order critical load of linear buckling analysis, and the corresponding displacement mode ϕ_1 is the first-order buckling mode. In this paper, ρ_1 is used as the load reference value of nonlinear buckling analysis. In the numerical analysis, the Riks arc length method is used to analyze the nonlinear buckling of the bearing assembly, and the critical load of nonlinear buckling is solved. The iterative equation is structured as follows:

$$\Delta U^i K_t = \lambda_{t+\Delta t} P - N_{t+\Delta t}^{i-1} \tag{5}$$

where ΔU^i is the iteration increment of current displacement, K_t is the tangent stiffness matrix of the structure at time t , $\lambda_{t+\Delta t}$ is $t + \Delta t$ load scale factor at time t , P is external load vector, and $N_{t+\Delta t}^{i-1}$ is $t + \Delta t$ Internal force vector of structural node at time t . To solve $\lambda_{t+\Delta t}$, additional constraint conditions need to be added, and the constraint equation is obtained by constraining the load level and displacement vector. The displacement increment ΔU^i is

combined with the load scale factor $\lambda_{t+\Delta t}$. Through the connection of arc length radius L , we can get:

$$\alpha (\Delta\lambda^i)^2 \|P\|^2 + \beta \|\Delta U^i\|^2 = (\Delta L)^2 \quad (6)$$

where $\|P\|$, $\|\Delta U^i\|$ are the two norms of external load vector and displacement increment, $\Delta\lambda^i$ is the load scale factor increment of the i 'th iteration, ΔL is the radius of the arc length increment, α , and β is the scale factor.

In the nonlinear buckling analysis, it is also necessary to introduce an initial perturbation value due to the influence of initial geometric imperfections. In general, the smaller the imperfection value, the closer the analysis result is to the actual buckling of the structure. In this paper, the average thickness is taken as a reference, and 1% and 10% of the average thickness are taken as the initial imperfection values.

5.1. Linear Eigenvalue Buckling Analysis

In the linear eigenvalue buckling analysis, considering the on-machine connection of the bearing assembly and the influence of the tensile load on the main bearing area, the stability of the bearing area is studied emphatically. Linear eigenvalue buckling analysis has created a step in Abaqus, and the procedure type of Buckle is used. Boundary conditions of the linear eigenvalue buckling analysis are established, as shown in Figure 11. All degrees of freedom are constrained at the fixed connection with the fuselage, and a fixed vertical unit load is applied in the bearing area. After the numerical analysis of eigenvalue buckling, the eigenvalue buckling of the first six order modes is solved.

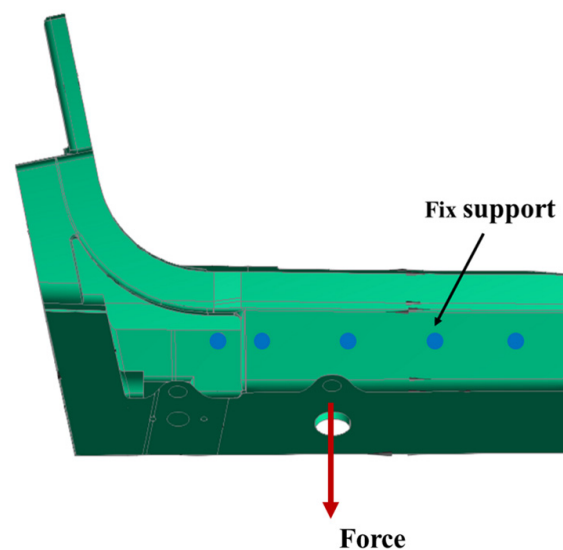


Figure 11. Boundary conditions of buckling analysis.

The first six eigenvalue buckling modes are shown in Figure 12, and the buckling eigenvalues are 464.9 KN, 483.4 KN, 491.1 KN, 491.2 KN, 985.3 KN, and 1000 KN, respectively. The first-order buckling mode deforms above the main bearing surface, the third-order buckling mode and the sixth-order buckling mode both deform in this area, but the eigenvalue is much larger than the first-order buckling eigenvalue. In this paper, the first-order buckling mode is selected as the initial geometric deformation of nonlinear buckling analysis, and the corresponding buckling eigenvalue is used as the load reference value of nonlinear buckling.

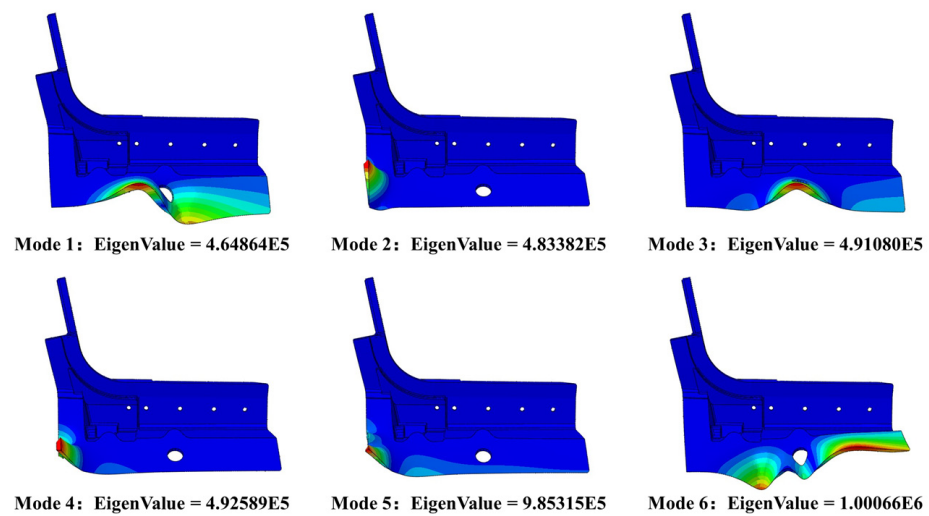


Figure 12. Eigenvalue buckling modes.

5.2. Nonlinear Buckling Analysis

The load-bearing components of aircraft are mostly composed of alloy metals with light weight and high strength. Under the load of more than a certain level, the components will undergo nonlinear deformation, which will produce plastic deformation. Due to the use and design factors of different component structures, structural instability may occur under loads less than this level, namely buckling. Nonlinear buckling analysis of the research object is considered. Nonlinear buckling analysis has created a step in Abaqus, and the procedure type of Buckle is used. By means of the first-order buckling mode and critical load obtained in the eigenvalue buckling calculation, the nonlinear buckling load is set to 464.9 KN. The Riks arc length method is used for nonlinear buckling analysis. The initial arc length is 0.01 mm, the maximum arc length is 0.1 mm, the minimum arc length is 0.001 mm, and the maximum number of iterations, with a total arc length of 1 mm, is 1000. Influence of geometric defects on the stability of the bearing assembly is considered. The 1% and 10% of the average thickness are taken as the initial imperfection values, respectively. The measured thickness of the bearing assembly is shown in Table 4. The nonlinear buckling of the bearing assembly, under no imperfection and initial imperfection, is calculated. After solving, the load-displacement curve on the main bearing surface is obtained as Figure 13. The critical load of nonlinear buckling without imperfection is 110.6 KN, the critical load of 1% initial imperfection is 108.4 KN, and the critical load of 10% initial imperfection is 106.2 KN. The critical load of nonlinear buckling under three conditions is only about 1/4 of the critical load of eigenvalue buckling, which shows that nonlinear buckling is more realistic than linear eigenvalue buckling. The three load values are not much different, indicating that the geometric defects of the bearing assembly are not obvious for nonlinear buckling and have certain structural stability.

Table 4. The measured thickness of the bearing assembly.

	D_{\min} (mm)	D_{\max} (mm)	D_{mid} (mm)	D_m (mm)
1	3.411	17.723	5.002	4.979
2	3.396	17.704	5.037	5.011
3	3.421	17.733	4.994	4.882
mean value	3.409	17.720	5.011	4.957

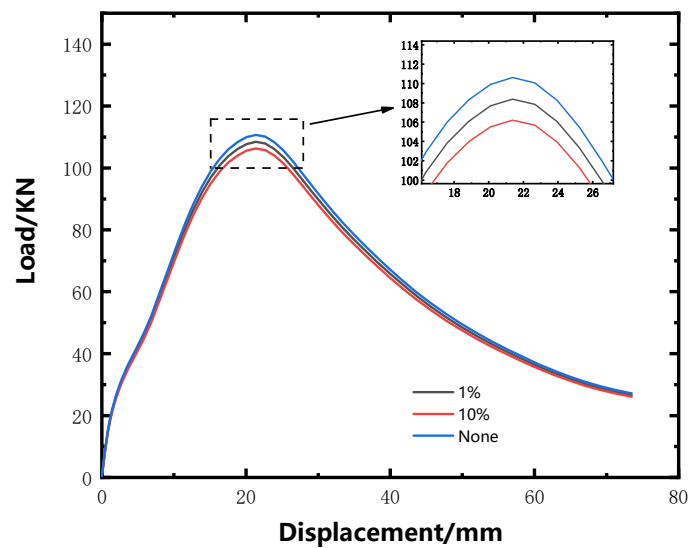


Figure 13. The load-displacement curve.

In the absence of disturbance, when the load in the load-bearing area of the load-bearing assembly reaches the critical load of nonlinear buckling, the displacement and deformation in the load-bearing area is 21.4 mm, and the corresponding stress situation is shown in Figure 14. The stress range on the load-bearing surface is 292.4~467.8 Mpa, which is less than the yield strength of the material; the stress in some areas reaches 701.7 Mpa, which exceeds the tensile strength of the material. At this time, the structure gradually loses stability. Since then, under the continuous load, the bearing capacity of the bearing area has decreased significantly, and the structure has entered the unstable state, which shows that it is necessary to consider the nonlinear buckling analysis.

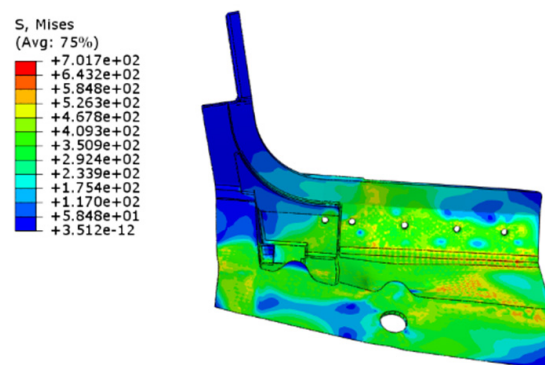


Figure 14. The stress situation of nonlinear buckling.

The stress curves of five nodes are extracted from the bearing surface area, and the node position is shown in Figure 15. The stress curves of nodes A to E are shown in Figure 16. Before reaching the critical load, the stress amplitude of nodes A, B, and C rises rapidly, and then, the stress level of the three points remains roughly unchanged. The stress of node E and node D increases with the load, and the stress at node D rises faster. However, when the load reaches the critical load, the stress levels of nodes E and D are smaller than those of nodes A, B, and C. From the results of stress analysis, when optimizing the structural strength, the structural strength of nodes A, B, and C should be considered emphatically, which improves the strength of the outer edge of the bearing area, as shown in Figure 17.



Figure 15. A–E is node position.

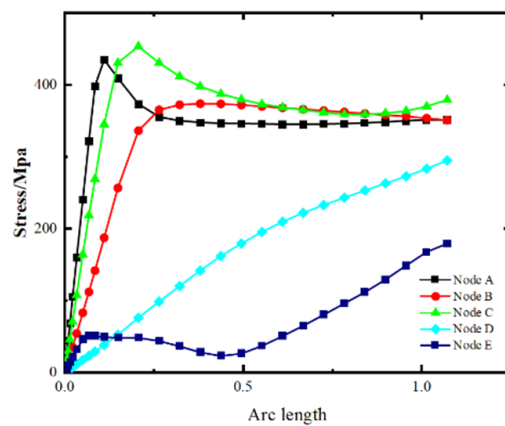


Figure 16. Stress curves of nodes A to E.

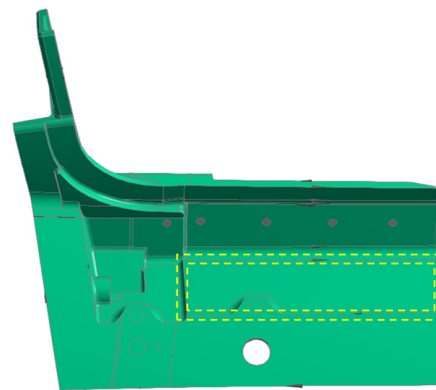


Figure 17. Outer edge of the bearing area.

6. Discussion

- (1) Strength test specification with 30.151 KN test load is used for strength analysis, and a reasonable strength test fixture is designed and manufactured. Numerical analysis results show that the stress level of the bearing area of the bearing component is about 425.3 Mpa, which is less than the yield strength of the material. Comparing the experimental value of the selected strain sensor S6 position with the numerical analysis results, the error is within 2.5%, indicating the effectiveness of the numerical analysis, and the structural strength of the bearing parts meets the requirements and has certain static strength stability. The stress value of the connection area of the test piece exceeds the yield strength $\sigma_{0.2}$, and strain of edge of the test piece is larger than other areas can be the further optimally designed in terms of structure strength.

- (2) The linear eigenvalue buckling analysis is used to solve the first six buckling orders of the bearing assembly, and the first-order buckling mode and the corresponding critical load 464.9 KN are obtained, respectively. The critical load value is the load value of nonlinear buckling through reference. The disturbance value is introduced in the nonlinear buckling analysis, and the critical load values of nonlinear buckling without perturbation, 1% initial imperfection, and 10% initial imperfection are 110.6 KN, 108.4 KN, and 106.2 KN, respectively. The three are about 1/4 of the critical load value of linear eigenvalue buckling, but the three critical load values are not much different, indicating that the geometric imperfections of the bearing parts are not obvious for nonlinear buckling and have certain structural stability. When the load exceeds the critical load value of nonlinear buckling, the displacement deformation of the bearing area reaches 21.4 mm, and the structure enters the instability state, indicating the necessity of considering nonlinear buckling analysis.
- (3) The strength test load, 30.151 KN, is about 27.3% of the critical load of nonlinear buckling, 110.6 KN. By analyzing the load loading of this large span, the stress range and deformation of the structural strength performance and the instability of the bearing member are summarized, which can provide the reference for the structural strength optimization design of the bearing member by using strength analysis and buckling analysis.

Author Contributions: Conceptualization, D.Z.; Supervision, D.Z.; Writing—review & editing, D.Z.; Investigation, G.Z.; Writing—original draft, G.Z.; Data curation, Y.C.; Methodology, Y.C. All authors have read and agreed to the published version of the manuscript.

Funding: This research received no external funding.

Institutional Review Board Statement: Not applicable.

Informed Consent Statement: Not applicable.

Data Availability Statement: The data presented in this study cannot be shared at this time as the data also forms part of an ongoing study.

Conflicts of Interest: The authors declare that they have no conflict of interest in this work. The funders had no role in the design of the study; in the collection, analyses, or interpretation of data; in the writing of the manuscript, or in the decision to publish the results.

References

1. Rizzi, A. Modeling and simulating aircraft stability and control—The SimSAC project. *J. Prog. Aerosp. Sci.* **2011**, *47*, 573–588. [[CrossRef](#)]
2. Ditemz, S.F. Failure analysis of aircraft main landing gear cylinder support. *J. Eng. Fail. Anal.* **2021**, *129*, 105711. [[CrossRef](#)]
3. Li, Z.; Wang, J.; Deng, F. Strength analysis and experimental verification of composite fuselage panels. *J. Chin. J. Aeronaut.* **2020**, *41*, 13.
4. Gupta, A.; Soni, V.; Shah, D.; Lakdawala, A. Generative design of main landing gear for a remote-controlled aircraft. *J. Mater. Today Proc.* **2023**, *in press*. [[CrossRef](#)]
5. Kilimtzidis, S. Efficient structural optimisation of composite materials aircraft wings. *J. Compos. Struct.* **2023**, *303*, 116268. [[CrossRef](#)]
6. Sun, X. A methodology for constructing the aircraft design schema. *J. Chin. J. Aeronaut.* **2023**, *in press*. [[CrossRef](#)]
7. Li, T. A multi-dimensional lagrange multiplier method to identify the load distribution on 3D special-shaped surface in the strength analysis of aircraft structure. *J. Int. J. Comput. Methods* **2023**, *ahead of print*. [[CrossRef](#)]
8. Cao, Q.; Wang, Y.; Yao, N.; He, G.; Chen, Z.; Zhang, G.; Tian, Z.; Wu, X. Development and application of strength design technology of advanced carrier-based aircraft. *J. Acta Aeronaut. Astronaut. Sin.* **2021**, *42*, 525793.
9. *HB 7713-2002*; Aviation Industry Standard of the People's Republic of China. General Requirements of Static Strength Test for Aircraft Structure. National Defense Science, Technology and Industry Commission: Beijing, China, 2002.
10. Chang, N.; Xu, R.; Chen, X.; Yang, J.; Li, Y. Design method for strength/durability preliminary structure optimization. *J. Acta Aeronaut. Astronaut. Sin.* **2021**, *42*, 524389.
11. Li, X.; Shao, F.; Zhu, Z.; Hu, Z.; Li, P. Design and strength test of lightweight T joints for ships. *J. Ship Mech.* **2018**, *22*, 454–463.
12. Aftb, S.G.; Sirajuddin, B.; Sreedhara, E.; Ganesh, A.; Ramesh Babu, N.; Kiran, S.A. Finite element analysis of a passenger aircraft landing gear for structural and fatigue safety. *J. Mater. Today* **2022**, *54*, 152–158. [[CrossRef](#)]

13. Xun, Y.; Li, Y. Approximate calculation method for buckling load of integral sub-stiffened panels. *J. Beijing Univ. Aeronaut. Astronaut.* **2015**, *41*, 6.
14. Khajehdezfuly, A.; Poorveis, D.; Nazarinia, S. Comparison between linear and nonlinear buckling loads of FGM cylindrical panel with cutout. *Int. J. Non-Linear Mech.* **2023**, *150*, 104361. [[CrossRef](#)]
15. Jáger, B.; Dunai, L. Nonlinear imperfect analysis of corrugated web beams subjected to lateral-torsional buckling. *J. Eng. Struct.* **2021**, *245*, 11288. [[CrossRef](#)]
16. Hinojosa, J.; Allix, O.; Guidault, P.-A.; Cresta, P. Domain decomposition methods with nonlinear localization for the buckling and post-buckling analyses of large structures. *J. Adv. Eng. Softw.* **2014**, *70*, 13–14. [[CrossRef](#)]
17. Pi, Y.L.; Bradford, M.A. Nonlinear analysis and buckling of shallow arches with unequal rotational end restraints. *J. Eng. Struct.* **2013**, *46*, 615–630. [[CrossRef](#)]

Disclaimer/Publisher's Note: The statements, opinions and data contained in all publications are solely those of the individual author(s) and contributor(s) and not of MDPI and/or the editor(s). MDPI and/or the editor(s) disclaim responsibility for any injury to people or property resulting from any ideas, methods, instructions or products referred to in the content.